Bioorganic & Medicinal Chemistry Letters xxx (2016) xxx–xxx

Contents lists available at ScienceDirect

Bioorganic & Medicinal Chemistry Letters

journal homepage: www.elsevier.com/locate/bmcl

Dioxol and dihydrodioxin analogs of 2- and 3-phenylacetonitriles as potent anti-cancer agents with nanomolar activity against a variety of human cancer cells

Nikhil R. Madadi [a], Amit Ketkar [b], Narsimha R. Penthala [a], April C. L. Bostian [b], Robert L. Eoff [b], Peter A. Crooks [a,*]

[a] Department of Pharmaceutical Sciences, College of Pharmacy, University of Arkansas for Medical Sciences, Little Rock, AR 72205, USA
[b] Department of Biochemistry and Molecular Biology, College of Medicine, University of Arkansas for Medical Sciences, Little Rock, AR 72205, USA

ARTICLE INFO

Article history:
Received 23 February 2016
Revised 15 March 2016
Accepted 16 March 2016
Available online xxxx

Keywords:
3,4-Methylenedioxycyanostilbenes
3,4-Ethylenedioxycyanostilbenes
Synthesis of cyanostilbenes
Anti-cancer activity
Molecular docking studies

ABSTRACT

A small library of (*Z*)-2-(benzo[*d*][1,3]dioxol-5-yl) and (*Z*)-2,3-dihydrobenzo[*b*][1,4]dioxin-6-yl analogs of 2- and 3-phenylacetonitriles has been synthesized and evaluated for their anti-cancer activities against a panel of 60 human cancer cell lines. The dihydrodioxin analog **3j** and dioxol analogs **5e** and **7e** exhibited the most potent anti-cancer activity of all the analogs synthesized in this study, with GI_{50} values of <100 nM against almost all of the cell lines in the human cancer cell panel. Of these three, only compound **3j** inhibited tubulin polymerization to any degree in vitro. The binding modes of **3j** and the structurally related tubulin-inhibitor **DMU-212** were determined by virtual docking studies with tubulin dimer. Compound **3j** docked at the colchicine-binding site at the dimer interface of tubulin. The Full-Fitness (FF) score of **3j** was observed to be substantially higher than **DMU-212**, which agrees well with the observed anti-cancer potency (GI_{50} values). The mechanism by which dioxol analogs **5e** and **7e** exert their cytotoxic effects remains unknown at this stage, but it is unlikely that they affect tubulin dynamics. Nevertheless, these findings suggest that both dioxol and dihydrodioxin analogs of phenylacrylonitrile may have potential for development as clinical candidates to treat a variety of human cancers.

In 1987, the US National Cancer Institute (NCI) identified the *cis*-stilbene analog, combretastatin A-4 (CA-4; Fig. 1, structure A), as the most potent anti-cancer agent of all the natural combretastatins isolated from the African bush willow, *Combretum caffrum*.[1] Early work showed that CA-4 targets tubulin and inhibits the proliferation of both murine and human cancer cells.[2] Unfortunately, subsequent reports have indicated that CA-4 possesses unfavorable properties, such as isomerization to the less active *trans*-stilbene isomer (Fig. 1, structure B) in solution, low water-solubility and vascular disruption,[3–5] which has precluded its development as a potential clinical candidate. Efforts to improve the drug-likeness properties of CA-4 have resulted in the discovery of a water-soluble prodrug, CA-4P, which is currently being evaluated in phase II/III clinical trials for activity in anaplastic thyroid carcinoma, non-small cell lung cancer, and ovarian cancer in combination with conventional standard of care cytotoxic drugs that include paclitaxel, carboplatin, and the antiangiogenic agent, brevacizumab.[6]

Recently our laboratory has reported on some novel *trans*-CA-4 (Fig. 1, structure B) analogs as potent inhibitors of tubulin polymerization with growth inhibitory activities superior to *cis*-CA-4.[4,5] These molecules can also be considered as structural analogs of resveratrol (Fig. 1, structure C), and include the anti-cancer agent **DMU-212** (Fig. 1, structure D), which binds to the colchicine binding site on tubulin. Our work has demonstrated that a trans double bond bearing a nitrile moiety can improve chemical stability and can serve as an effective replacement for the *cis*-olefinic moiety in CA-4 and its analogs.[5] More recently, we have reported on a series of diphenyl, 2-benzothio phenyl/phenyl, and 2-quinolinyl/phenyl acrylonitrile derivatives (Fig. 1, structures E, F, and G respectively) as potent anti-proliferative agents that have potential as anti-tubulin therapeutics for treatment of both solid and hematological tumors.[7]

In our current studies we have now synthesized a small library of thirty one substituted phenylacrylonitrile analogs that incorporate benzo[*d*][1,3]dioxol-5-yl and 2,3-dihydrobenzo[*b*][1,4]dioxin-6-yl moieties and have evaluated them against a panel of 60 human tumor cell lines. The most potent analogs identified have been evaluated as inhibitors of tubulin polymerization.

* Corresponding author. Tel.: +1 501 686 6495; fax: +1 501 686 6057.
E-mail address: pacrooks@uams.edu (P.A. Crooks).

http://dx.doi.org/10.1016/j.bmcl.2016.03.068
0960-894X/

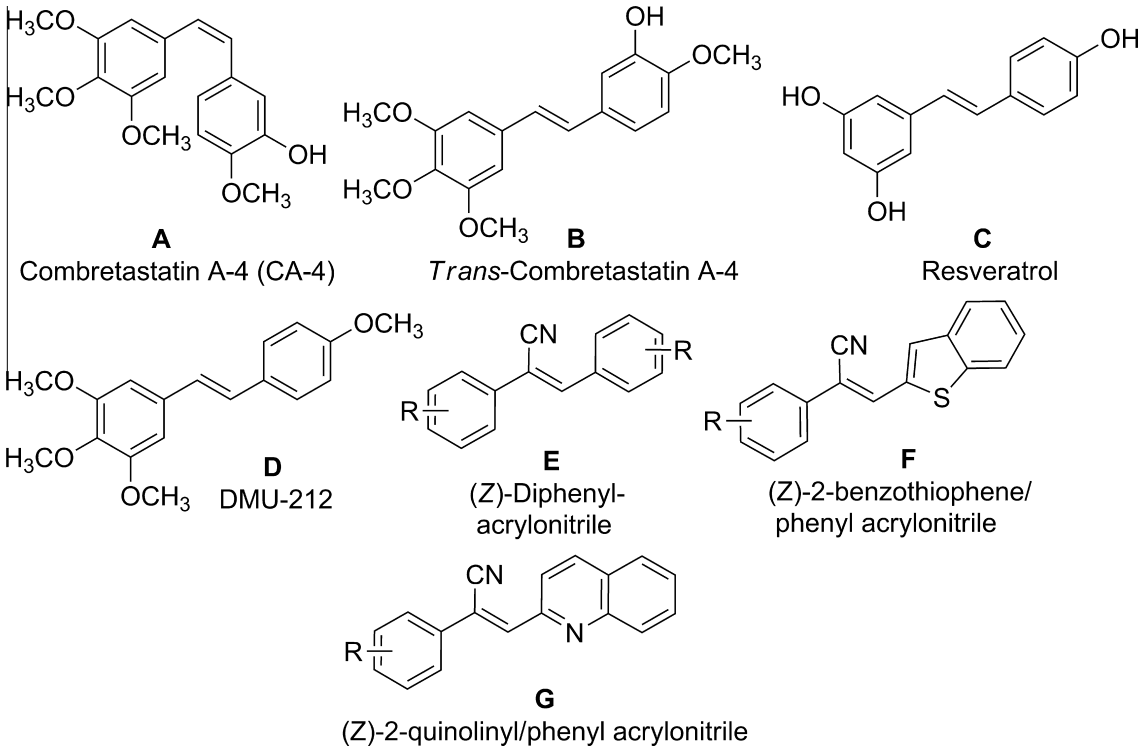

Figure 1. Structures of combretastatin A-4 (CA-4), *trans*-CA-4, **DMU-212**, (*Z*)-diphenyl, (*Z*)-2-benzothiophene/phenyl, and (*Z*)-2-quinolinyl/phenyl acrylonitrile derivatives.

An initial series of eleven (*Z*)-3-(benzo[*d*][1,3]dioxol-5-yl)-2-phenylacrylonitrile (**3a–3e**) and (*Z*)-3-(2,3-dihydrobenzo[*b*][1,4]-dioxin-6-yl-2-phenylacrylonitrile **(3f–3k)** analogs were synthesized by reacting benzo-[*d*][1,3]dioxole-5-carbaldehyde (**2a**) or 2,3-dihydrobenzo[*b*][1,4]dioxine-6-carbaldehyde (**2b**) with an appropriately substituted phenylacetonitrile (**1a–1h**) at reflux temperature in 5% sodium methoxide/methanol to yield the desired compounds in yields ranging from 70% to 95% (Scheme 1).[7,8]

A second series of twelve substituted (*Z*)-2-(benzo[*d*][1,3] dioxol-5-yl)-3-phenylacrylonitrile analogs (**5a–5l**) were synthesized by reacting appropriately substituted aromatic aldehydes (**4a–4l**) with 2-(benzo[*d*][1,3]dioxol-5-yl)acetonitrile (**1i**) at reflux temperature in 5% sodium methoxide/methanol. The reaction was carried out as described previously[7] for analogs **3a**–**3k**[8] to yield the desired compound in yields ranging from 80% to 90% (Scheme 2).

A third series of substituted (*Z*)-2-(benzo[*d*][1,3]dioxol-5-yl)-3-phenyl acrylonitrile analogs (**7a–7h**) were synthesized by reacting appropriate substituted aromatic and hetero aromatic aldehydes (**6a–6h**) with 2-(benzo[*d*][1,3]dioxol-5-yl)acetonitrile (**1i**) at reflux temperature in 5% sodium methoxide/methanol. The reaction was carried out as described previously[7] for analogs **3a**–**3k**[8] to yield the desired compound in yields ranging from 80% to 90% (Scheme 3).

The NCI employs an effective triage system for the submitted compounds based on duplicates already screened and ADME algorithm results, prior to selecting them for initial single dose and subsequent five dose screening assays.[9] The in vitro screening of the above compounds was carried out utilizing the procedure described by Rubinstein et al.[9–11] Of the thirty one phenylacetoni-

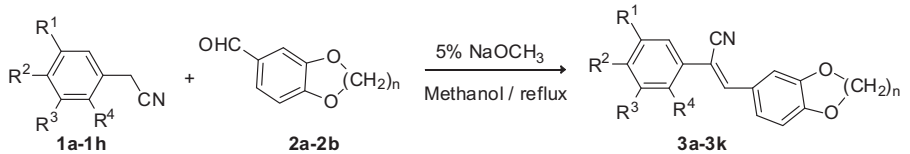

1a: $R^1 = R^3 = OCH_3$, $R^2 = R^4 =$ H
1b: $R^1 = R^2 = R^3 = OCH_3$, R^4 = H
1c: $R^1 = R^2 = R^3$ = H, $R^4 = OCH_3$
1d: $R^1 = R^3 = R^4$ = H, $R^2 = NO_2$
1e: $R^1 = R^3 = R^4$ = H, $R^2 = OCH_3$
1f: $R^1 = R^2 = R^3 = R^4$ = H
1g: $R^1 = R^2 = R^3$ = H, $R^4 = CF_3$
1h: $R^1 = R^2 = OCH_3$, $R^3 = R^4$ = H

2a: n=1
2b: n=2

3a: $R^1 = R^3 = OCH_3$, $R^2 = R^4$ = H, n=1
3b: $R^1 = R^2 = R^3 = OCH_3$, R^4 = H, n=1
3c: $R^4 = OCH_3$, $R^1 = R^2 = R^3$ = H, n=1
3d: $R^2 = NO_2$, $R^1 = R^3 = R^4$ = H, n=1
3e: $R^2 = OCH_3$, $R^1 = R^3 = R^4$ = H, n=1
3f: $R^1 = R^2 = R^3 = R^4$ = H, n=2
3g: $R^1 = R^3$ = H, $R^4 = CF_3$, n=2
3h: $R^1 = R^2 = OCH_3$, $R^3 = R^4$ = H, n=2
3i: $R^1 = R^3 = R^4$ = H, $R^2 = OCH_3$, n=2
3j: $R^1 = R^2 = R^3 = OCH_3$, R^4 = H, n=2
3k: $R^2 = NO_2$, $R^1 = R^3 = R^4$ = H, n=2

Scheme 1. Synthesis of (*Z*)-2-(benzo[*d*][1,3]dioxol-5-yl)-2-phenylacrylonitrile (**3a–3e**) and (*Z*)-2,3-dihydrobenzo[*b*][1,4]dioxin-6-yl-2-phenylacrylonitrile **(3f–3k)** analogs.

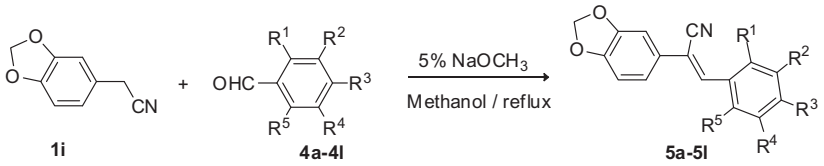

4a: R^2= R^3= R^4= OCH_3, R^1= R^5= H
4b: R^2 = R^4= OCH_3, R^1 = R^3 = R^5 = H
4c: R^2 = R^4= Br, R^1= R^3 = R^5 = H
4d: R^2 = R^4 = F, R^1 = R^3= R^5 = H
4e: R^3= OCH_3, R^1= R^2 = R^4 = R^5 = H
4f: R^2= R^3 = OCH_3, R^1= R^4 = R^5= H
4g: R^2 = R^3= Cl, R^1= R^4= R^5 = H
4h: R^1= R^5 = Cl, R^2= R^3 = R^4= H
4i: R^2 = Br, R^3= F, R^1= R^4 = R^5= H
4j: R^3 = R^5 = OCH_3, R^1 = R^2 = R^4 = H
4k: R^3 = R^5= Cl, R^1 = R^2 = R^4 = H
4l: R^3= R^4= OCH_3, R^5 = Cl, R^1= R^2= H

5a: R^2= R^3= R^4= OCH_3, R^1= R^5= H
5b: R^2 = R^4= OCH_3, R^1 = R^3 = R^5 = H
5c: R^2 = R^4= Br, R^1= R^3 = R^5 = H
5d: R^2 = R^4 = F, R^1 = R^3= R^5 = H
5e: R^3= OCH_3, R^1= R^2 = R^4 = R^5 = H
5f: R^2= R^3 = OCH_3, R^1= R^4 = R^5= H
5g: R^2 = R^3= Cl, R^1= R^4= R^5 = H
5h: R^1= R^5 = Cl, R^2= R^3 = R^4= H
5i: R^2 = Br, R^3= F, R^1= R^4 = R^5= H
5j: R^3 = R^5 = OCH_3, R^1 = R^2 = R^4 = H
5k: R^3 = R^5= Cl, R^1 = R^2 = R^4 = H
5l: R^3= R^4= OCH_3, R^5 = Cl, R^1= R^2= H

Scheme 2. Synthesis of substituted (*Z*)-2-(benzo[*d*][1,3]dioxol-5-yl)-3-phenylacrylonitrile analogs (**5a–5l**).

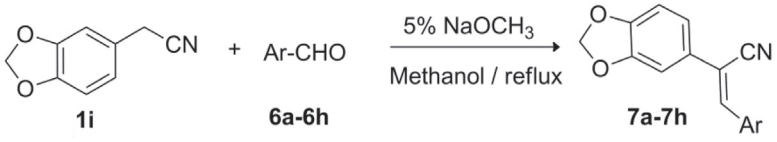

Compound	6a/7a	6b/7b	6c/7c	6d/7d	6e/7e	6f/7f	6g/7g	6h/7h
Ar								

Scheme 3. Synthesis of (*Z*)-2-(benzo[*d*][1,3]dioxol-5-yl-3-heteroarylacrylonitrile analogs (**7a–7h**).

trile analogs synthesized, fourteen analogs (**3e**, **3h–3j**, **5a–5h**, **5k**, **5l** and **7a–7h**) were selected and evaluated for anti-cancer activity against a panel of 60 human tumor cell lines. Compounds were initially screened at 10^{-5} M to determine growth inhibition (GI_{50}) (single dose results for compounds **3e**, **3h–3j**, **5a–5l**, **7a–7h** are provided in the supporting information). The 10 μM single dose screening results for these compounds are presented in the supplementary data section. From the 14 compounds selected for single dose screening, eight compounds (**3h–3j**, **5e**, **5j**, and **7c–7e**) showed promising anti-cancer activity and were selected for subsequent five dose studies.

Tables 1 and 2 provide the 50% Growth Inhibitory (GI_{50}) data from the five-dose study of the above eight compounds and for the positive control, **DMU-212**, a structurally related stilbene analog, against the panel of 60 human tumor cell lines. **DMU-212** is an anti-tubulin agent which has been shown to possess potent anti-proliferative/proapoptotic activities in a variety of cancer cells, including K562 (leukemia), HT29 (colo-rectal), and HePG2 (hepatoma) HeLa (cervical), LnCaP (prostate), HepG2 (hepatoma) and MCF-7 (breast) cancer cells.[12–14]

From the five dose studies of the (*Z*)-2,3-dihydro-benzo[*b*][1,4]-dioxin-6-yl-2-phenylacrylonitrile analogs **3h–3j** (Scheme 1), compound **3j** was found to be a very effective anti-cancer agent with an average GI_{50} value of 97 nM against all 60 human cancer cell lines in the panel. In particular, **3j** exhibited a GI_{50} value of 20 nM against cancer cell lines SF-295 (CNS), SF-539 (CNS), and MDA-MB-435 (melanoma) and a GI_{50} value of 30 nM against HCT-116 (colon), SNB-75 (CNS), M14 (melanoma), SK-MEL-5 (melanoma), UACC-62 (melanoma), NCI/ADR-RES (ovarian), A498 (renal) and MDA-MB-468 (breast) cancer cell lines. When the 3,4,5-methoxyphenyl group of compound **3j** was replaced with a 3,4-dimethoxyphenyl moiety (**3h**), the average GI_{50} values declined from 97 nM to 3.7 μM. Also, when the 3,4,5-trimethoxyphenyl group of compound **3j** was replaced with a 4-methoxyphenyl moiety (**3i**) the average GI_{50} values deteriorated even further (~50% of the GI_{50} values were >100 μM). The growth inhibition activities of analogs **3h**, **3i** and **3j** suggest that the presence of a 3,4,5-trimethoxyphenyl group affords significant anti-cancer activity against most of the human cancer cell lines in the panel.

From the five dose studies carried out on the (*Z*)-2-(benzo[*d*][1,3]dioxol-5-yl-3-arylacrylonitrile analogs **5e**, **5j**, and **7c–7e**, compounds **5e** and **7e** were the most potent anti-cancer agents in this series. Compound **7e** was particularly effective against three specific cancer cell lines: NCI-H522 (non-small cell lung), SNB-75 (CNS) and MDA-MB-435 (melanoma) with GI_{50} values of 20 nM and also exhibited GI_{50} values of 30 nM against HL-60(TB) (leukemia), SR (leukemia), COLO 205 (colon), HT29 (colon) and A498 (renal) cancer cell lines. Substitution of a 1-naphthyl or 4-methoxy-1-naphthyl moiety for the 2-benzthiophenyl moiety in **7e** resulted in significant loss of anti-cancer activity (i.e. compounds **7c** and **7d**, respectively, Table 2). Compound **5e** exhibited significant anti-cancer activity against HOP-62 (non-small cell lung) and MDA-MB-435 (melanoma) cancer cell lines with GI_{50} values of 30 nM, and afforded a GI_{50} value of 40 nM against K-562 (leukemia) and NCI-

Table 1
Growth inhibition (GI_{50}/μM)[a] data for compounds **3h–3j** and **DMU-212** against a panel of 60 human cancer cell lines

Panel/cell line	**3h** GI_{50} (μM)	**3i** GI_{50} (μM)	**3j** GI_{50} (μM)	**DMU-212** GI_{50} (μM)
Leukemia				
CCRF-CEM	3.76	>100	**0.21**	2.89
HL-60(TB)	2.07	>100	**0.04**	3.14
K-562	NA[b]	NA	NA	NA
MOLT-4	8.85	>100	**0.62**	3.22
RPMI-8226	4.81	>100	**0.06**	6.42
SR	**0.93**	2.76	**0.06**	3.93
Non-small cell lung cancer				
A549/ATCC	4.12	21.7	**0.06**	3.70
HOP-62	2.98	>100	**0.05**	3.14
HOP-92	9.64	>100	**0.12**	7.23
NCI-H23	6.61	>100	**0.16**	3.37
NCI-H522	2.80	>100	**0.05**	3.70
Colon cancer				
COLO 205	2.77	>100	**0.12**	2.07
HCC-2998	8.85	7.78	**0.14**	3.59
HCT-116	2.71	6.33	**0.03**	3.23
HCT-15	**0.73**	2.10	**0.04**	2.82
HT29	NA	NA	NA	2.32
KM12	1.59	4.26	**0.05**	3.63
SW-620	1.04	3.93	**0.04**	2.07
CNS cancer				
SF-268	5.38	>100	**0.11**	7.59
SF-295	2.49	10.6	**0.02**	2.18
SF-539	2.56	73.1	**0.02**	2.18
SNB-19	4.08	>100	**0.19**	4.85
SNB-75	2.16	21.9	**0.03**	1.88
U251	3.97	>100	**0.05**	3.07
Melanoma				
LOX IMVI	4.92	NA	**0.06**	4.89
M14	1.63	3.87	**0.03**	2.81
MDA-MB-435	**0.26**	**0.51**	**0.02**	1.04
SK-MEL-2	1.84	36.8	NA	3.95
SK-MEL-28	4.59	>100	**0.06**	3.86
SK-MEL-5	**0.84**	3.54	**0.03**	2.50
UACC-62	1.04	8.68	**0.03**	2.37
Ovarian cancer				
IGROV1	9.40	>100	**0.63**	5.29
OVCAR-3	2.16	37.1	**0.04**	3.45
OVCAR-4	11.2	24.9	**0.26**	4.00
NCI/ADR-RES	1.52	4.45	**0.03**	3.01
SK-OV-3	3.24	>100	**0.04**	3.34
Renal cancer				
786-0	3.88	35.8	**0.04**	5.42
A498	1.35	>100	**0.03**	**0.74**
ACHN	7.61	>100	**0.08**	4.51
CAKI-1	2.92	>100	**0.05**	3.00
UO-31	5.01	>100	NA	3.69
Prostate cancer				
PC-3	4.57	>100	**0.06**	3.22
DU-145	4.69	>100	**0.13**	4.23
Breast cancer				
MCF7	**0.86**	3.01	**0.04**	1.66
MDA-MB-231/ATCC	4.69	69.3	**0.17**	3.74
HS 578T	5.56	>100	**0.07**	3.09
MDA-MB-468	1.11	4.29	**0.03**	2.22

GI_{50} values <1 μM are bolded.
[a] GI_{50}: 50% growth inhibition, concentration of drug resulting in a 50% reduction in net protein increase compared with control cells.
[b] NA: not analyzed.

Table 2
Growth inhibition (GI_{50}/μM)[a] data for compounds **5e**, **5j**, and **7c–7e** against a panel of 60 human cancer cell types

Panel/cell line	**5e** GI_{50} (μM)	**5j** GI_{50} (μM)	**7c** GI_{50} (μM)	**7d** GI_{50} (μM)	**7e** GI_{50} (μM)
Leukemia					
CCRF-CEM	**0.25**	1.56	3.65	1.91	**0.05**
HL-60(TB)	**0.24**	1.49	3.50	1.57	**0.03**
K-562	**0.04**	**0.39**	**0.79**	**0.53**	**0.04**
MOLT-4	**0.45**	2.81	4.99	3.71	**0.07**
RPMI-8226	**0.49**	3.23	4.49	3.85	**0.19**
SR	**0.05**	**0.53**	1.60	5.44	**0.03**
Non-small cell lung cancer					
A549/ATCC	**0.27**	2.65	5.00	2.65	**0.09**
HOP-62	**0.30**	3.30	3.77	2.14	**0.07**
HOP-92	4.22	7.42	4.55	12.0	17.00
NCI-H23	**0.86**	6.33	6.45	5.09	**0.32**
NCI-H522	**0.04**	2.58	2.89	2.37	**0.02**
Colon cancer					
COLO 205	**0.14**	1.59	2.58	1.61	**0.03**
HCC-2998	5.26	11.9	11.0	5.42	**0.27**
HCT-116	**0.22**	2.68	3.72	2.41	**0.04**
HCT-15	**0.07**	**0.87**	1.77	**0.75**	**0.04**
HT29	**0.06**	**0.71**	3.02	1.60	**0.03**
KM12	**0.07**	2.25	3.77	2.39	**0.05**
SW-620	**0.12**	1.23	3.72	**0.72**	**0.05**
CNS cancer					
SF-268	**0.73**	9.36	8.99	9.34	1.64
SF-295	**0.20**	1.75	2.96	1.91	**0.04**
SF-539	**0.25**	1.61	2.71	1.58	**0.04**
SNB-19	**0.75**	6.95	6.29	4.24	**0.23**
SNB-75	NA[b]	NA	2.45	1.14	**0.02**
U251	**0.43**	3.59	3.85	2.71	**0.06**
Melanoma					
LOX IMVI	**0.57**	5.33	4.22	3.96	**0.05**
M14	**0.12**	1.32	3.13	1.68	**0.04**
MDA-MB-435	**0.03**	**0.30**	**0.43**	**0.31**	**0.02**
SK-MEL-2	**0.21**	**0.72**	3.18	2.90	**0.04**
SK-MEL-28	**0.45**	4.47	5.84	4.52	**0.24**
SK-MEL-5	**0.21**	2.58	3.20	1.52	**0.06**
UACC-62	**0.59**	2.32	2.63	1.51	**0.06**
Ovarian cancer					
IGROV1	3.60	8.80	5.95	4.07	**0.09**
OVCAR-3	**0.27**	3.10	4.18	3.04	**0.04**
OVCAR-4	NA	1.65	8.25	3.79	1.27
NCI/ADR-RES	**0.08**	2.41	2.52	1.65	**0.04**
SK-OV-3	**0.40**	2.75	3.58	2.35	**0.06**
Renal cancer					
786-0	18.90	4.93	5.62	4.38	**0.88**
A498	**0.20**	1.33	1.17	**0.41**	**0.03**
ACHN	**0.52**	4.92	4.52	4.24	**0.06**
CAKI-1	NA	NA	4.18	2.06	**0.05**
UO-31	**0.58**	6.66	6.48	6.24	**0.08**
Prostate cancer					
PC-3	**0.32**	3.03	5.52	3.04	**0.06**
DU-145	**0.59**	3.62	6.94	3.49	**0.21**
Breast cancer					
MCF7	**0.08**	**0.85**	1.99	**0.61**	**0.09**
MDA-MB-231/ATCC	2.11	3.36	5.11	2.43	**0.18**
HS 578T	**0.46**	3.62	3.54	2.63	**0.08**
MDA-MB-468	**0.28**	**0.69**	2.11	**0.51**	**0.38**

GI_{50} values <1 μM are bolded.
[a] GI_{50}: 50% growth inhibition, concentration of drug resulting in a 50% reduction in net protein increase compared with control cells.
[b] NA: not analyzed.

H522 (non-small cell lung) cancer cells. The anti-cancer activity declined significantly (only ~25% of the GI_{50} values were <1 μM) when the 4-methoxyphenyl group of compound **5e** was replaced with a 2,4-dimethoxyphenyl moiety (**5j**).

In vitro tubulin polymerization experiments were performed, as described previously[15] in order to test the ability of compounds **3j**, **5e** and **7e** to exert their cytotoxic effects through inhibition of tubulin dynamics. The tubulin polymerization assay measures changes over time in optical density (O.D.) at 340 nM. An increase

Please cite this article in press as: Madadi, N. R.; et al. *Bioorg. Med. Chem. Lett.* (2016), http://dx.doi.org/10.1016/j.bmcl.2016.03.068

in the O.D. results from tubulin polymerization. The resulting curve typically exhibits three phases: an initial nucleation phase, a polymerization phase, and a steady-state phase where there is slow depolymerization of tubulin as the GTP substrate is depleted (Fig. 2A).

Compound **3j** appeared to affect both the rapid polymerization phase and the slow depolymerization phase in a concentration-dependent manner (Fig. 2B and C). The tubulin polymerization rate decreased from 8.6 (±0.4) × 10^{-4} A.U.s/s for the DMSO control reaction to 6.9 (±0.9) × 10^{-4} A.U.s/s ($P = 0.083$) and 2.0 (±1.2) × 10^{-4} A.U.s/s ($P < 0.0001$) in the presence of 10 μM and 100 μM **3j**, respectively (where $n = 3–6$ experiments and values reported represent the mean ± std. error) (Fig. 2B). The tubulin depolymerization rate increased from 1.3 (±0.1) × 10^{-5} A.U.s/s for the DMSO control reaction to 1.6 (± 0.2) × 10^{-5} A.U.s/s ($P = 0.11$) and 3.2 (±0.3) × 10^{-5} A.U.s/s ($P < 0.0001$) in the presence of 10 μM and 100 μM **3j**, respectively (where $n = 3–6$ experiments and values reported represent the mean ± std. error) (Fig. 2C).

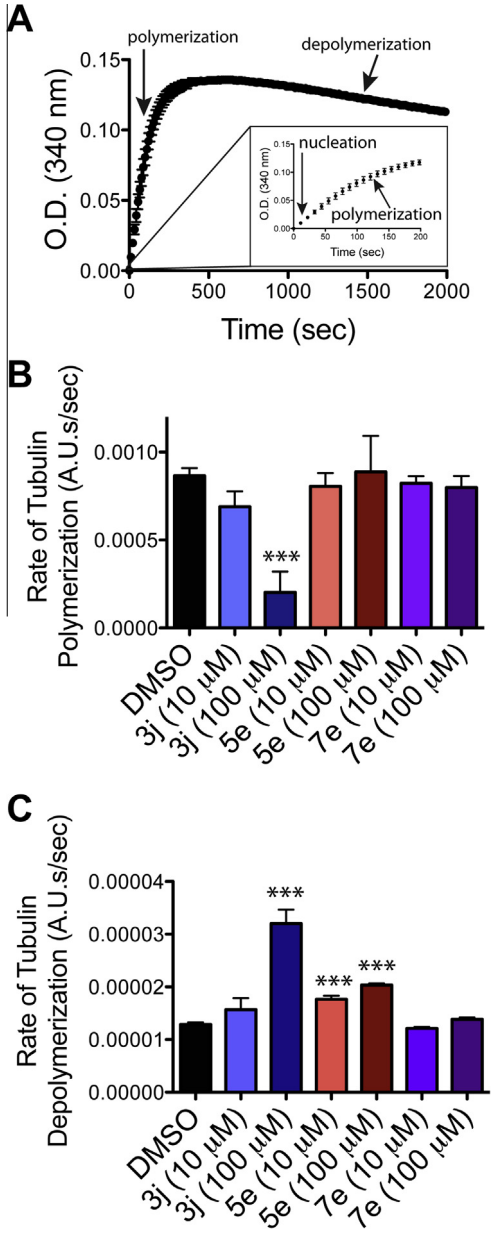

Figure 2. In vitro tubulin polymerization in the presence of **3j**, **5e**, and **7e**. Panel A. Representative tubulin polymerization results. The reaction was initiated by raising the temperature of tubulin from 4 °C to 37 °C and then monitoring changes in O.D. at 340 nm. The three phases of the tubulin polymerization assay are noted. The rate of tubulin polymerization (Panel B) and depolymerization (Panel C) was measured in the presence of the indicated concentrations of **3j**, **5e**, and **7e**. DMSO served as a control reaction. Asterisks represent *P* values, which were calculated using a Student's t-test.

Compound **5e**, on the other hand, did not alter the initial rate of polymerization to any degree, changing from 8.6 (±0.4) × 10^{-4} A.U.s/s for the DMSO control reaction to 8.0 (± 0.7) × 10^{-4} A.U.s/s ($P = 0.51$) and 8.9 (±2.0) × 10^{-4} A.U.s/s ($P = 0.87$) in the presence of 10 μM and 100 μM **5e**, respectively (where $n = 3–6$ experiments and values reported represent the mean ± std. error) (Fig. 2B). Compound **5e** exhibited a slightly stronger effect on tubulin depolymerization, as the tubulin depolymerization rate increased from 1.3 (±0.1) × 10^{-5} A.U.s/s for the DMSO control reaction to 1.8 (±0.6) × 10^{-5} A.U.s/s ($P = 0.0003$) and 2.0 (±0.3) × 10^{-5} A.U.s/s ($P < 0.0001$) in the presence of 10 μM and 100 μM **5e**, respectively (where $n = 3–6$ experiments and values reported represent the mean ± std. error) (Fig. 2C). Finally, compound **7e** did not alter tubulin dynamics in any measurable way (Fig. 2B and C). Taken together, it would appear that while **3j** is able to actively disrupt tubulin dynamics, **5e** only destabilizes tubulin after GTP is depleted, and **7e** is without effect.

Among the most potent anti-cancer compounds identified in this study, only **3j** showed a significant effect in our tubulin polymerization assay. In order to determine the binding mode of compounds **3j** and to compare it with that of the known tubulin-inhibitor **DMU-212**, virtual docking of these compounds was performed with the tubulin dimer. All docking studies were performed using SwissDock, as described earlier.[15] Briefly, atomic coordinates of all the ligands were generated using MarvinSketch (ChemAxon), and coordinates for tubulin were derived from the crystal structure PDB 1SA0. All coordinates files were prepared for docking using UCSF-Chimera, and submitted for docking to the SwissDock server. Resulting binding modes were ranked based on Full-Fitness (FF) scores generated by SwissDock, and the top-scoring poses for each compound were examined in detail manually to identify their interactions with tubulin.

Both **3j** and **DMU-212** docked at the colchicine-binding site at the dimer interface of tubulin (Fig. 3A). Table 3 shows the docking (FF) scores for these compounds. Interestingly, the FF score for the tubulin inhibitor **DMU-212** was observed to be significantly lower (−2198.7 kcals/mol) than compound **3j** in our docking studies.

None of the compounds make any polar contacts with any residues of tubulin. Both **3j** and **DMU-212** are stabilized through van der Waals' interactions at the colchicine-binding site on tubulin. **DMU-212** interacts with residues of β-tubulin only, whereas compound **3j** makes additional van der Waals' contacts with four residues of α-tubulin, besides sharing all the β-tubulin contacts made by **DMU-212** (Fig. 3B). This would explain the low FF score of **DMU-212** as compared to **3j**.

In conclusion, a series of (*Z*)-2-(benzo[*d*][1,3]dioxol-5-yl) and (*Z*)-2,3-dihydrobenzo[*b*][1,4]dioxin-6-yl analogs of 2- and 3-phenylacetonitriles has been synthesized and evaluated for their anti-cancer activities against a panel of 60 human cancer cell lines. Eight compounds (**3h–3j, 5e, 5j,** and **7c–7e**) were identified as molecules of interest from a single dose anti-cancer screening assay. These compounds were then evaluated for dose-dependent growth inhibition and cytotoxicity against the 60 human cancer cell panel. From the eight compounds selected, analogs **3j** and **7e** exhibited the most potent anti-cancer activity with GI_{50} values of <100 nM against a significant number of cell lines in the panel. Compound **5e** exhibited GI_{50} values <1 μM against most of the human cancer cell lines in the panel. These analogs also showed superior growth inhibition when compared to the structurally related tubulin inhibitor, **DMU-212**. Tubulin polymerization was inhibited in vitro by **3j**, and molecular docking studies

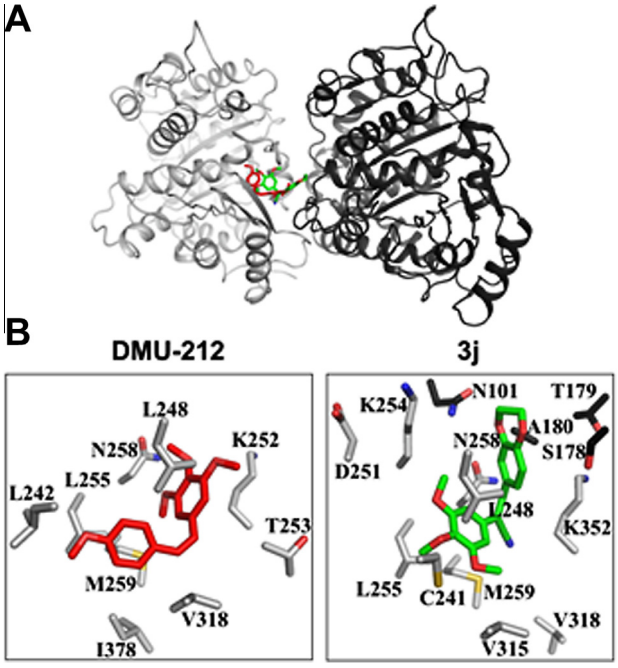

Figure 3. Docking poses at the colchicine binding site of tubulin. a. The tubulin dimer is shown as a cartoon, with α-tubulin in *black* and β-tubulin in *light gray*. Top binding poses of the compounds **3j** (*red*) and **DMU-212** (*green*) are shown at the dimer interface. b. Zoomed view for the top poses of **DMU-212** (*red*) and **3j** (*green*) are shown at the colchicine-binding site of tubulin in each panel. Residues of tubulin involved in van der Waals' interactions with the two compounds are labeled in each panel.

Table 3
Docking scores of **3j** and **DMU-212** with tubulin

Compound	FF score (kcal/mol)
3j	−4217.6
DMU-212	−2198.7

demonstrated that **3j** has a higher affinity for the colchicine-binding site on tubulin when compared to **DMU-212**. Compounds **5e** and **7e** do not appear to exert cytotoxicity through inhibition of tubulin dynamics.

It should be noted that tubulin inhibitor **3j** is a member of the (*Z*)-2,3-dihydrobenzo[*b*]-[1,4]dioxin-6-yl-2-arylacrylonitrile series of analogs, whereas compounds **5e** and **7e**, belong to the (*Z*)-2-(benzo[*d*][1,3]dioxol-5-yl-3-arylacrylonitrile series of analogs. Molecular docking studies show that the 3-(3,4-ethylenedioxyphenyl)-acetonitrile moiety in the dihydrodioxin analog **3j** is recognized by tubulin and similar to DMU-212 binds to the colchicine binding site on tubulin. Dioxol compounds **5e** and **7e** both contain a 2-(3,4-methylenedioxyphenyl)-acetonitrile moiety, and are potent anticancer agents but exhibit little or no inhibition of tubulin polymerization. The mechanism by which **5e** and **7e** exert their cytotoxic effects remains unknown at this stage, but it is unlikely that they affect tubulin dynamics. Nevertheless, the results from this study suggest that (*Z*)-2-(benzo[*d*][1,3]-dioxol-5-yl) and (*Z*)-2,3-dihydrobenzo[*b*][1,4]-dioxin-6-yl analogs of 2- and 3-arylacetonitriles may have potential for development as clinical candidates to treat a variety of human cancers.

Acknowledgements

We are grateful to the NCI/NIH, United States (Grant Number CA 183895 and COBRE Award Number P20GM109005), to the Arkansas Research Alliance Scholar award (to P.A.C.) and to the NCI drug screening program.

Supplementary data

Supplementary data associated with this article can be found, in the online version, at http://dx.doi.org/10.1016/j.bmcl.2016.03.068.

References and notes

1. Pettit, G. R.; Singh, S. B.; Niven, M. L.; Hamel, E.; Schmidt, J. M. *J. Nat. Prod.* **1987**, *50*, 119.
2. Pettit, G. R.; Singh, S. B.; Hamel, E.; Lin, C. M.; Alberts, D. S.; Garcia-Kendall, D. *Experientia* **1989**, *45*, 209.
3. Greene, L. M.; Wang, S.; O'Boyle, N. M.; Bright, S. A.; Reid, J. E.; Kelly, P.; Meegan, M. J.; Zisterer, D. M. *Oncol. Rep.* **2013**, *29*, 2451.
4. Madadi, N. R.; Penthala, N. R.; Song, L.; Hendrickson, H. P.; Crooks, P. A. *Tetrahedron Lett.* **2014**, *55*, 4207.
5. Penthala, N. R.; Janganati, V.; Bommagani, S.; Crooks, P. A. *Med. Chem. Commun.* **2014**, *5*, 886.
6. Lee, L.; Robb, L. M.; Lee, M.; Davis, R.; Mackay, H.; Chavda, S.; Babu, B.; O'Brien, E. L.; Risinger, A. L.; Mooberry, S. L.; Lee, M. *J. Med. Chem.* **2010**, *53*, 325.
7. Penthala, N. R.; Sonar, V. N.; Horn, J.; Leggas, M.; Yadlapalli, J. S.; Crooks, P. A. *Med. Chem. Commun.* **2013**, *4*, 1073.
8. *General synthetic procedure synthesis of (Z)-2-(benzo [d][1,3]dioxol-5-yl) and (Z)-2,3-dihydrobenzo[b] [1,4]dioxin-6-yl analogs of 2- and 3-phenylacetonitriles* (**3a**–**3k**, **5a**–**5l**, and **7a**–**7h**): the aromatic carbaldehyde (1 mole) and the appropriate substituted phenylacetonitrile (1.1 mol equiv) were added to 5% sodium methoxide in methanol and the mixture was stirred at reflux temperature for 2–3 h. The resulting solid was filtered off, washed with water, and finally washed with cold methanol. The obtained crude solid was recrystallized from methanol to afford the desired product as a pure crystalline solid. The characterization data for the active compounds is given in reference section.
9. Rubinstein, L. V.; Shoemaker, R. H.; Paull, K. D.; Simon, R. M.; Tosini, S.; Skehan, P.; Scudiero, D. A.; Monks, A.; Boyd, M. R. *J. Natl. Cancer Inst.* **1990**, *82*, 1113.
10. Penthala, N. R.; Yerramreddy, T. R.; Madadi, N. R.; Crooks, P. A. *Bioorg. Med. Chem. Lett.* **2010**, *20*, 4468.
11. Janganati, V.; Penthala, N. R.; Madadi, N. R.; Chen, Z.; Crooks, P. A. *Bioorg. Med. Chem. Lett.* **2014**, *24*, 3499.
12. Androutsopoulos, V. P.; Ruparelia, K. C.; Papakyriakou, A.; Filippakis, H.; Tsatsakis, A. M.; Spandidos, D. A. *Eur. J. Med. Chem.* **2011**, *46*, 2586.
13. Sale, S.; Verschoyle, R. D.; Boocock, D.; Jones, D. J. L.; Wilsher, N.; Ruparelia, K. C.; Potter, G. A.; Farmer, P. B.; Steward, W. P.; Gescher, A. J. *Br. J. Cancer* **2004**, *90*, 736.
14. Madadi, N. R. C.; Lett, P. A. *Drug Design Discovery* **2015**, *12*, 521.
15. Madadi, N. R.; Penthala, N. R.; Howk, K.; Ketkar, A.; Eoff, R. L.; Borrelli, M. J.; Crooks, P. A. *Eur. J. Med. Chem.* **2015**, *103*, 123.